Chapter 1

Fluids Background

1.1 Boussinesq approximation

The Navier-Stokes equations are the mathematical equations that govern the evolution of fluid flow. In the context of the ocean and atmosphere, the Navier-Stokes equations, along with an equation of state, provide good models of the evolution of fluid flow e.g. Batchelor [5]. For our purposes, however, these equations are too general and an approximation, called the Boussinesq approximation, can be made which results in a simplified version of the Navier-Stokes equations:

$$\frac{\partial \boldsymbol{u}}{\partial t} + \boldsymbol{u} \cdot \nabla \boldsymbol{u} = -\frac{1}{\rho_0} \nabla p - \frac{\rho' g}{\rho_0} \hat{\boldsymbol{e}}_z + \nu \nabla^2 \boldsymbol{u} \tag{1.1}$$

$$\nabla \cdot \boldsymbol{u} = 0 \tag{1.2}$$

$$\frac{\partial \rho'}{\partial t} + \boldsymbol{u} \cdot \nabla \rho' = \kappa \nabla^2 \rho' - \frac{\partial \bar{\rho}}{\partial z} w \tag{1.3}$$

where we have the following dimensional variables

- $\mathbf{u}(x, y, z, t) = (u(x, y, z, t), v(x, y, z, t), w(x, y, z, t))$ is the velocity field in the x, y, z-directions directions respectively,
- $p(x, y, z, t)$ is the pressure field,
- $\rho(x, y, z, t)$ is the density,
- ρ_0 is a constant reference density,

- $\bar{\rho}(z)$ is a linear mean density profile,
- $\rho'(x, y, z, t)$ is a perturbation density,
- g is the gravitational constant,
- ν is the constant kinematic velocity,
- κ is the constant molecular diffusivity.

Equations (1.1)-(1.3) are a set of five coupled partial differential equations for the unknowns $\mathbf{u}, p, \rho$. Herein, we will refer to equation (1.1) as the velocity equations, equation (1.2) as the continuity equation, and equation (1.3) as the density equation. An additional useful quantity to define is the buoyancy frequency or the Brunt-Vaisala frequency which is defined as

$$N^2 = -\frac{g}{\rho_0}\frac{d\bar{\rho}}{dz}. \tag{1.4}$$

Note that we have included a negative sign because we assume that the linear density profile is decreasing. In the literature a positive sign also appears in the definition of the buoyancy frequency. Both definitions, however, will lead to the same conclusions.

A rigorous derivation of the Boussinesq equation is quite delicate and we provide a brief overview of the derivation. A complete derivation, along with many of the subtleties can be found in numerous books such as [23, 42, 44] and a rigorous mathematical derivation in (Spiegel and Veronis). The Navier-Stokes equations for a compressible Newtonian fluid can be written as

$$\rho\frac{D\boldsymbol{u}}{Dt} = -\nabla p + \rho\mathbf{g} + \mu\nabla^2\boldsymbol{u}, \tag{1.5}$$

$$\frac{1}{\rho}\frac{D\rho}{Dt} + \nabla\cdot\boldsymbol{u} = 0. \tag{1.6}$$

The Boussinesq equations are based off the following approximation to the density equation [23, 44]

$$\rho(\boldsymbol{x}, t) = \rho_0 + \bar{\rho}(z) + \rho'(\boldsymbol{x}, t) \tag{1.7}$$

where we assume that $\bar{\rho}(z), \rho' \ll \rho_0$. In other words variations to the density are small compared to a reference density.

The first approximation we make is replacing the mass continuity equation with the more simple incompressible equation $\nabla \cdot \boldsymbol{u} = 0$. However, since we are interested in a fluid with non-constant density, it is not as simple as setting $\rho = \rho_0$. The approximation we make is that even though the density is non-constant, it is approximately in hydrostatic balance [44]. Thermodynamically [23], this means that density varies as

$$\frac{\delta\rho}{\rho} = -\alpha\delta T \tag{1.8}$$

where α is the thermal expansion coefficient, which for many gases is on the order of 10^{-3} K^{-1} and fluids 10^{-4} K^{-1} [23]. If the variation in temperature $\delta T \sim 10$ K, which is a reasonable approximation for many applications of oceanic and atmospheric modeling, then $\alpha\delta T \ll 1$. Comparing the material derivative and the velocity term in the conservation equation yields, assuming a characteristic velocity and length scales of U and L [23],

$$\frac{(1/\rho)(D\rho/Dt)}{\nabla \cdot \mathbf{u}} \sim \frac{(U/\rho)\delta\rho/L}{U/L} = \frac{\delta\rho}{\rho} \ll 1. \tag{1.9}$$

Thus we can replace the mass continuity with the "incompressability condition".

We have simplified the equations of motion, however we still have five unknowns with only four equations. To get a fifth equation, we again appeal to thermodynamics. It can be shown that given the above density approximation, the thermodynamic equation of state of the density [44] can be written as

$$\frac{D\rho'}{Dt} - N^2 w = \kappa\nabla^2\rho' \tag{1.10}$$

which closes the system. Finally, in the momentum equation, if we plug in the density approximation we obtain

$$\left(1 + \frac{\bar{\rho}}{\rho_0} + \frac{\rho'}{\rho_0}\right)\frac{D\boldsymbol{u}}{Dt} = -\frac{1}{\rho_0}\nabla p + \left(1 + \frac{\bar{\rho}}{\rho_0} + \frac{\rho'}{\rho_0}\right)\mathbf{g} + \mu\nabla^2\boldsymbol{u}. \tag{1.11}$$

The terms multiplying the interial terms are tiny and can be neglected [23]. The terms multiplied gravity need to be treated more carefully because of the hydrostatic balance condition. The resulting equation is [23, 44] is

$$\frac{\partial\boldsymbol{u}}{\partial t} + \boldsymbol{u}\cdot\nabla\boldsymbol{u} = -\frac{1}{\rho_0}\nabla p - \frac{\rho' g}{\rho_0}\hat{\boldsymbol{e}}_z + \nu\nabla^2\boldsymbol{u}. \tag{1.12}$$

Thus we have derived the so-called Boussinesq approximation.

1.2 Linear Stability Analysis

The stability of flows has a long and rich history within fluid dynamics. The classic experiment into the stability of fluid flow is that of Reynolds [37]. In this experiment, Reynolds injected dye into the laminar flow through a pipe. By varying the velocity of the flow through the pipe Reynolds observed various effects. If the velocity was sufficiently low, Reynolds was able to observe "a beautiful straight line through the tube". At slightly higher velocities, the straight line behaviour remained near the initial part of the pipe but further down "the streak would shift about the tube, but there was no appearance of sinuosity". By increasing the velocity significantly, the dye would again initially remain straight near the initial part of the tube, but instead of shifting about the tube "the colour band would all at once mix up with the surrounding water, and fill the rest of the tube with a mass of coloured water". (add image from Acheson?)

What Reynolds observed was the transition and breakdown of a flow into turbulence. Through careful observation, he determined that the dimensionless quantity that governed the behaviour of the flow was the Reynolds number

$$Re = \frac{UL}{\nu}, \tag{1.13}$$

a number which, as discussed above represents the ratio between the inertial and viscous terms in the Navier-Stokes equations. Reynolds found that if $Re < 13000$ then the flow would remain stable.

The natural question to ask is to whether we can predict such criteria for any given flow. Ideally, given information about a certain flow, one would be like to be able to determine how the fluid will evolve based on various parameters of the flow, such as viscosity, temperature, or velocity. Unfortunately this task has not been achieved in general and there is no known way to determine such criteria for any arbitrary flow. This is due to the complicated nonlinear behaviour of the Navier-Stokes equations which makes devising a general algorithm for this task incredibly difficult. Tackling this goal in general is immensely difficult and beyond current mathematics, indeed it is not even known whether or not in three dimensions given an initial condition a solution even exists for all times.

Thus, to proceed, a simplying approach must be derived. In order to do this, consider the following idea. Let $(\boldsymbol{u}_0, p)$ denote a basic state that solves the Navier-Stokes equations and let $(\boldsymbol{u}', p')$ denote a small unknown perturbation such that $|\boldsymbol{u}', p'| \ll |\boldsymbol{u}_0, p|$. Mathematically this means

$$\boldsymbol{u}(\boldsymbol{x}, t) = \boldsymbol{u}_0(\boldsymbol{x}, t) + \boldsymbol{u}'(\boldsymbol{x}, t), \qquad p(\boldsymbol{x}, t) = p_0(\boldsymbol{x}, t) + p'(\boldsymbol{x}, t). \tag{1.14}$$

Now let us plug (1.14) into the Navier-Stokes equations and expand, dropping the $(\boldsymbol{x}, t)$ notation,

$$\frac{\partial \boldsymbol{u}_0}{\partial t} + \frac{\partial \boldsymbol{u}'}{\partial t} + (\boldsymbol{u}_0 + \boldsymbol{u}') \cdot \nabla(\boldsymbol{u}_0 + \boldsymbol{u}') = -\frac{1}{\rho_0}\nabla(p_0 + p') + \nu\nabla^2(\boldsymbol{u}_0 + \boldsymbol{u}'), \tag{1.15}$$

$$\nabla \cdot \boldsymbol{u}_0 + \nabla \cdot \boldsymbol{u}' = 0. \tag{1.16}$$

Expanding out the advection term yields

$$(\boldsymbol{u}_0 + \boldsymbol{u}') \cdot \nabla(\boldsymbol{u}_0 + \boldsymbol{u}') = \boldsymbol{u}_0 \cdot \nabla \boldsymbol{u}_0 + \boldsymbol{u}_0 \cdot \nabla \boldsymbol{u}' + \boldsymbol{u}' \cdot \nabla \boldsymbol{u}_0 + \boldsymbol{u}' \cdot \nabla \boldsymbol{u}' \tag{1.17}$$

$$= \boldsymbol{u}_0 \cdot \nabla \boldsymbol{u}_0 + \boldsymbol{u}_0 \cdot \nabla \boldsymbol{u}' + \boldsymbol{u}' \cdot \nabla \boldsymbol{u}_0 + \mathcal{O}(\boldsymbol{u}'^2), \tag{1.18}$$

where we have written the $\boldsymbol{u}' \cdot \nabla \boldsymbol{u}'$ term has $\mathcal{O}(\boldsymbol{u}'^2)$ because this term is of order $\boldsymbol{u}'$ squared, which we assume to be small. Now recall that the basic state $\boldsymbol{u}_0$ solves the Navier-Stokes equations. Thus in (1.16) there are terms that depend just on $\boldsymbol{u}_0$ and they will vanish by definition of it being a solution to the Navier-Stokes equations. Thus we now have that

$$\frac{\partial \boldsymbol{u}'}{\partial t} + \boldsymbol{u}_0 \cdot \nabla \boldsymbol{u}' + \boldsymbol{u}' \cdot \nabla \boldsymbol{u}_0 + \mathcal{O}(\boldsymbol{u}'^2) = -\frac{1}{\rho_0}\nabla p' + \nu\nabla^2 \boldsymbol{u}' \tag{1.19}$$

$$\nabla \cdot \boldsymbol{u}' = 0. \tag{1.20}$$

So far, the equation above is exact and we have just supressed the quadratic nonlinear term in the Big-O notation. Now the critical assumption we make is that because $\boldsymbol{u}'$ is small relative to the basic state $\boldsymbol{u}_0$, $\boldsymbol{u}'^2$ is even smaller and thus is negligible. In other words, we are throwing away the quadratic nonlinearity of the perturbation term because it assumed to be small.

Now making the approximation that $\mathcal{O}(\boldsymbol{u}'^2)$ is small we obtain

$$\frac{\partial \boldsymbol{u}'}{\partial t} + \boldsymbol{u}_0 \cdot \nabla \boldsymbol{u}' + \boldsymbol{u}' \cdot \nabla \boldsymbol{u}_0 = -\frac{1}{\rho_0}\nabla p' + \nu\nabla^2 \boldsymbol{u}' \tag{1.21}$$

$$\nabla \cdot \boldsymbol{u}' = 0. \tag{1.22}$$

The above set of equations is linear which means they are more amenable to analytical and numerical techniques.

To illustrate the usefulness in this approach, we demonstrate an example of the general idea of linear stability and apply it to the formulation of the experiment of Reynolds. This is a standard example and we follow the derivation of [18]. It will also elucidate the key features of linear stability analysis that we will use throughout this thesis.

The first simplifying assumption we make is that the basic state $\boldsymbol{u}_0 = U(z)\hat{\boldsymbol{e}}_x$, a parallel shear flow, which simplifies the above equations to

$$\frac{\partial \boldsymbol{u}'}{\partial t} + U\frac{\partial \boldsymbol{u}}{\partial x} + w'\frac{dU}{dz}\hat{\boldsymbol{e}}_x = -\frac{1}{\rho_0}\nabla p' + \nu\nabla^2\boldsymbol{u}' \tag{1.23}$$

$$\nabla \cdot \boldsymbol{u}' = 0. \tag{1.24}$$

If we had considered the Euler equations instead of the Navier-Stokes equations, we would have the same equations as above except with $\nu = 0$. Despite this seemingly simple modification, the resulting equation is very different. When the invsicid equations are considered, there are many elegant results about the stability of the flow that can be derived for the special case of parallel shear flow. For example, the Rayleigh's inflection point theorem states that a necessary condition for instability is that the basic velocity profile should have an inflection point[18]. Unfortunately, many of the results for inviscid flow theory do not hold for viscous flow theory. A complete discussion of this result and its generalisation, among other theorems, can be found in [18, 23].

Since the resulting set of equations is a set of coupled linear equations, the solution set is complex exponentials. Thus, the next natural step is to expand the solution as Fourier modes

$$\boldsymbol{u}'(\boldsymbol{x}, t) = \hat{\boldsymbol{u}}(z)e^{i(\alpha x + \beta y - \alpha c t)} \tag{1.25}$$

$$p'(\boldsymbol{x}, t) = \hat{p}(z)e^{i(\alpha x + \beta y - \alpha c t)} \tag{1.26}$$

where we take the real part of the above solutions. We require that the solution remains bounded as $x, y \Rightarrow \pm\infty$ which means that α, β must remain real. For c, however, we let it remain an arbitrary complex number $c = c_r + ic_i$. Depending on the sign of c_i the result will either decay or grown exponentially as time goes to infinity. We thus associate stability with $c_i \leq 0$ and instability with $c_i > 0$. Hence, if we are able to solve the above system and derive a criteria for the value of c_i we will be able to derive some criteria for the stability of the flow.

Plugging in the above Fourier expansions into the linear equations would yield an eigenvalue-eigenvector problem with α, β, c, Re being undetermined. From there we could apply numerical linear algebra routines to solve numerically for various Re, α, β and obtain a stability curve for c. However, a result due to Squire allows us to simplify the problem significantly. Squire's theorem states that to obtain the minimum critical Reynolds number it is sufficient to cosndier only two-dimesnional disturbances[18]. In other words, for every three dimensional mode, there is a more unstable two dimensional eigenmode. A proof is provided in [18]. Because we only need to consider two dimensional flow, the unknown

velocity $\boldsymbol{u}'$ can be rewritten in terms of the stream function $\psi'(x, y, z, t)$. Another advantage of writing the equations in terms of the stream function is that the pressure is eliminated further reducing the number of unknowns.

Expanding ψ' as a complex exponential and denoting ϕ as the amplitude of the stream function and $D = d/dz$, the linear equations can be re-written as a single equation,

$$(D^2 - \alpha^2)^2\phi = (i\alpha\mathrm{Re})(U - c)(D^2 - \alpha^2)\phi - (i\alpha\mathrm{Re})U''\phi \tag{1.27}$$

along with the appropriate boundary conditions. This equation is known as the Orr-Sommerfeld equation and has a rich history in the development of fluid mechanics. A comprehensive discussion of the various methods of solving this equation and others like it using techniques such as WKB theory, asymptotics, and perturbation theory, is contained in [18, 45, 14].

This simple derivation has resulted in a single equation with three unknowns α, c, Re and by choosing different Re and α, we can determine a criteria for c. Although much work has been done at the beginning of the 20th century to derive approximate solutions to the Orr-Sommerfeld equation, numerically it is very easy to solve. We can reformulate the above equation as a generalised eigenvalue problem for a given parallel shear flow and solve the problem rather easily on a computer[41] and we can find that the condition for stability is $Re \sim 5500$, although the question of how valuable this is debatable[41].

Linear stability is a useful technique for determining whether or not a given flow is stable, however it is important to not forget the underlying assumptions. Since we are explicitly assuming that $|\boldsymbol{u}'| \ll |\boldsymbol{u}_0|$ the resulting linear equations are only valid when this is the case. As we shall see in numerical simulations, this assumption is not necessarily valid at all times. If viscous dissipation is neglected, the Euler equations conserve energy. If there is viscous dissipation then the Navier-Stokes only approximately conserve energy, but even if we included a complicated mechanism for molecular dissipation, the resulting equations would still have to conserve energy, as long as there is no external forcing and thus if we were very careful and measured everything the total amount of energy in the system would remain constant. However we have stated that if $c_i > 0$ then we have exponential growth. Clearly, as time advances, this gets infinitely large very quickly which implies that the perturbation will grow unbounded exponentially. This violates conservation of energy, since the total amount of energy of the pertrubation is growing, and violates the assumption that the perturbation is small.

The reason this occurs in linear stability analysis is simple: we implicitly assume that the basic state remains undisturbed, i.e. that the perturbations are small enough so they do not change the basic state. This means, when running a numerical simulation, the

perturbation is able to grow in time while the basic state remains unchanged. Thus we can think of the basic state as continuously pumping in energy into the perturbation state, allowing it to grow unbounded. Physically, this is not the case. In a full nonlinear simulation, the basic state does not remain unchanged and as the perturbation begins to grow, the basic state loses energy and changes and eventually reaches a point where we can no longer assume the perturbation is small compared to the basic state. Thus we have a breakdown of the linear theory and would need to turn to a nonlinear theory to continue our modeling.

However, despite violating conservation of energy, linear stability still provides useful information. Even though the individual eigenmodes grow exponentially, which eigenmodes are growing gives insight into what mechanisms are causing the growth. As we shall see, linear stability theory tells us what length scales dominate in the transition to turbulence in a stratified fluid. Given this information, it is possible to assume a certain scaling of the full nonlinear equations which can provide us with a potential simplified model to study the problem of turbulence in stratified fluids.

So far, we have studied the Navier-Stokes equations directly instead of, the perhaps more promising, Euler equations. Recall the Euler equations arise by setting the viscosity to 0 or letting the Reynolds number go to infinity. The Euler equations also have some other nicer features, such as explicit conservation of energy which might provide a useful potential invariant that we can exploit in the study of stability and turbulence.

To motivate the possible us of the Euler equations, consider the observation that turbulence is very often observed at a high Reynolds number. In the atmosphere for example, the Reynolds number is on the order of $10^8 - 10^9$ or higher. Since the inverse of the Reynolds number appears in front of the diffusion term, it seems reasonable to instead ignore the diffusion term since the coefficient is $\mathcal{O}(\mathrm{Re}^{-1}) \ll 1, Re \gg 1$. This would be a mistake. This is because the limit $Re \to \infty$ is a singular limit. Consider the following simplified model which arises in the study of boundary layers of shear bounded wall flow[14, 1, 23]

$$\epsilon y'' - y = 0 \qquad y(0) = 0, \qquad y(1) = 1. \tag{1.28}$$

If we set $\epsilon = 0$ we would obtain the equation

$$-y = 0 \qquad y(0) = 0, y(1) = 1. \tag{1.29}$$

which clearly has no solution that satisfies the boundary conditions. If we tried a perturbation expansion of the form $y(x) = \sum_{n=0} y_n(x)\epsilon^n$ we would get nowhere because the lowest order term does not exist. If we solve the full equation, we see the problem with

setting $\epsilon = 0$,

$$y(x) = \frac{e^{x/\epsilon} - 1}{e^{1/\epsilon} - 1}. \tag{1.30}$$

In this equation, we cannot set $\epsilon = 0$ because that results in a singular limit. Thus regardless of how small we choose ϵ, there will be a thin layer, called the boundary layer, which is essential to the fluid flow. For a discussion of techniques in singular perturbation theory in terms of the linear stability of the Navier-Stokes equations see [18, 45]. Hence, even though it seems reasonable to neglect the diffusion term to study instability and turbulence, it is not as a promising avenue as one might first expect. In one sense, this singular limit of the Navier-Stokes equations contributes to making turbulence a very difficult problem to investigate analytically and numerically.

Finally, the experimental investigation into instability of fluids and the transition to turbulence produces very appealing images which really illustrate the beauty of fluid dynamics and the reader is recommended to peruse the coffee table book by Van Dyke [46] which illustrates many images from experiments of the classical results in stability theory.

1.3 The Zigzag Instability

1.3.1 A Brief History of Vortex Instabilties

The origin of vortex instabilities begins with Lord Kelvin who in 1880 studied perturbations to columnar vortices and determined that they were stable. For the next 90 years, the theory of vortex instability remained relatively quiet until the field was re-ignited by the investigations Crow [15]. Motivated by engineering applications, Crow was an aeronautical engineer, he discovered that for long wavelength perturbations of a pair of counter-rotating vortices that there was a symmetric deformation of the vortices. This worked extended a few years later by Widnall et. al [52] to small wavelength perturbations. Further investigations into small wavelength perturbations were carried out by numerous others e.g. [32, 43]. It was noticed in these studies that the streamlines of the vortex became elliptical when perturbed. Motivated by this, Pierrehumbert [36] investigated the simple case of a single 2D elliptical vortex subject to a constant 3D pertubation. Extensions to this elliptical model were done by Bayly [4] and Waleffe [51] and led to this instability being called the elliptical instability. A complete and detailed history of the elliptical instability, including derivations and results of the above papers and nonlinear investigations, is presented in the review by Kerswell [22]. Most of the investigations into the elliptical instability were

concerned with unstratified flow, but an investigations by Miyazaki and Fukumoto [31] showed with sufficient stratification, the elliptical instability is surpressed.

1.3.2 Discovery of the Zigzag Instability

Experiments into this elliptical instability by Leweke and Williamson [25] led Billant, Brancher, and Chomaz [6] to investigate the stability of a three dimensional vortex pair which, as we shall discuss below, provides a good model of the experimental setup. Initially this work was unstratified and confirmed the existence of the elliptical instability. However, following up this work, Billant and Chomaz added in the effects of stratification and discovered a new type of instability at small scales that was distinct from the elliptical instability. They labeled this new instability the "zigzag instability" due to its zigzag-like structure, as we shall see below. In a series of three papers they investigated experimentally[7], theoretically[8], and numerically [9] the evolution of a pair of columnar vortices in a stratified tank.

First Billant and Chomaz investigated the zigzag instability experimentally [7]. To do this, they investigated a columnar vortex pair created by a pair of flaps in a tank of stratified fluid. We now briefly discuss their experimental procedure since it provides important motivation for the resulting numerical study.

In order to study the effects of stratification on the evolution of vortices, they first needs to create the vortices. To do this, they used a pair of motor-controlled flaps whose initial angle and closing time could be controlled precisely by a computer. When the flaps were closed, a pair of counter-rotating vortices was produced. They found that the important determining factor in the creation of the vortices was the angle of the flaps. If the angle was too small, additional vortices created when the flaps finally stopped closing were being advected by the dipole and causing spurious instability. For large angles fluid that was initially inbetween the flaps was being injected in the flow and again causing spurious oscillations. In order to balance out these effects, an angle of 14° was chosen. Additionally, to enforce the emergence of the zigzag instability, tape was applied to the flaps in order to force certain wavenumbers of the evolving flow, see Figure 8 of [7] for the importance of forcing.

After fixing the seperation angle they found that by varying the closing time of the flaps, the velocity of the pair of vortices could be changed. Interestingly, the decay of the vortices, roughly 90s, was independent of the closing time of the flaps. This variation in the velocity determined the experimental parameters for the experiment.

The two important dimensional parameters in this experiment were the horizontal Froude number

$$F_h = \frac{U}{NR} \tag{1.31}$$

and the Reynolds numbers

$$\mathrm{Re} = \frac{UR}{\nu} \tag{1.32}$$

where U is the propagating velocity of the dipole as above, R is the riadus of the dipole, ν is the viscosity of the tank, and N is the buoyancy frequency. Here the viscosity ν and the radius R were fixed by experimental conditions and could not be varied. Thus the only parameters that could be varied were N and U. Since the buoyancy frequency was more difficult to vary, as changing it required draining and refilling the tank, only four stratifications were considered ranging from $N = 1.26$ rad s^{-1} to $N = 1.97$ rad s^{-1}. Thus the parameter that was easy to control was the initial velocity U. Because U shows up in both dimensionless numbers, changing U resulted in the changing of both numbers, i.e. they are directly related by the following relationship

$$\mathrm{Re} = F_h \frac{NR^2}{\nu} \tag{1.33}$$

and for the given stratification numbers the ranges for the Froude number were between $0.10 - 0.23$ and for the Reynolds number $200 - 450$.

To determine a theoretical model of the dipole, they computed the FFT of the measured vorticity in order to determine the streamfunction. They found that there was a linear fit between the vorticity ω and the streamfunction ψ such that $\omega = k^2\psi$ where $k^2 = 1.15\mathrm{cm}^{-2}$ which, as we will show below, corresponds to a columnar Lamb-Chaplygin dipole.

Figure 1.1 demonstrates the evolution for the zigzag instability for $F_h = 0.19$ and $Re = 365$. The structure of the vortices displays a zigzag like structure. Additionally, the anistrophy between the vertical and horizontal directions is quite clear. The periodic behaviour of the vortex pair is also evident.

Following up the experimental work, Billant and Chomaz provided a theoretical account of the zigzag instability starting from the Bousinessq equations [8]. We will only discuss the main result of the paper as the paper is a very technical and long perturbation analysis. In the paper, they investigated the limit where $F_{h,v} = U/L_{h,v}N \ll 1$ and found that the zigzag motion was accounted for by combination of translation and rotation, which agrees

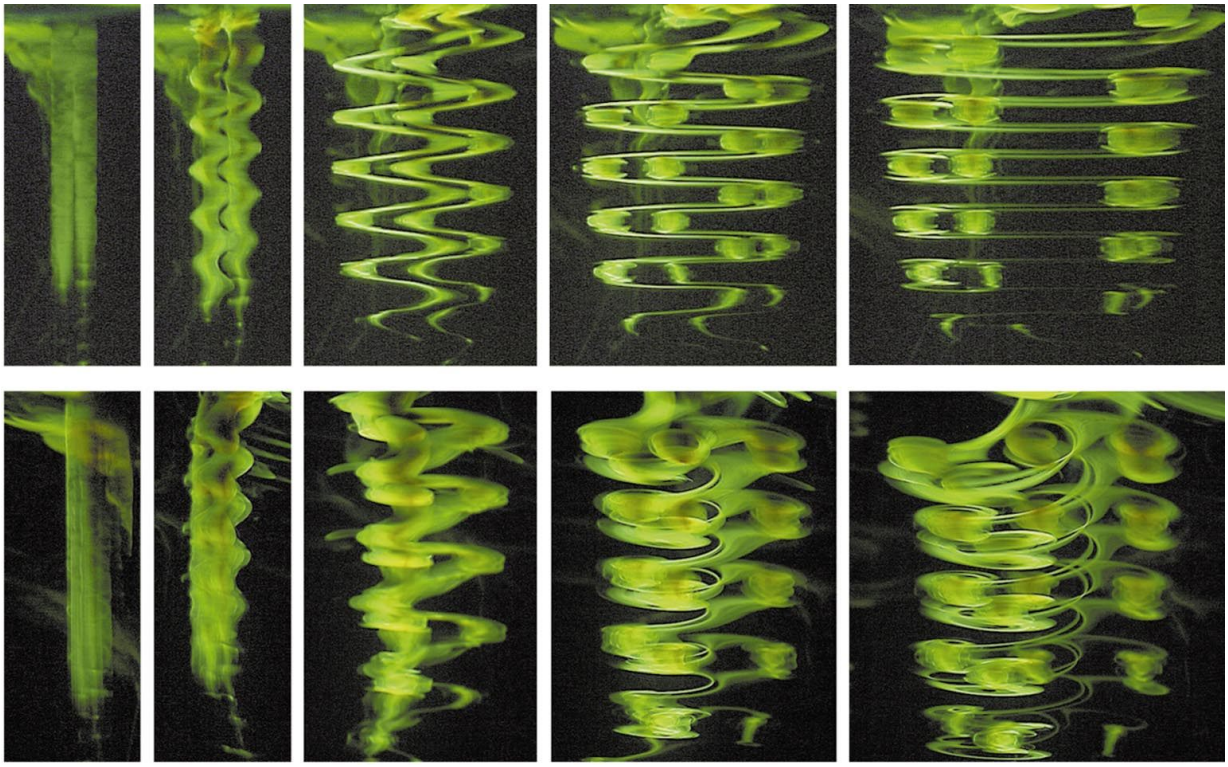

Figure 1.1: (get permission from JFM for picture + caption) A sequence of frontal (top) and side (bottom) views showing the growth of the zigzag instability for $F_h = 0.19$ and $Re = 365$. From left to right the pictures are taken at $7, 36, 75, 109, 121, 176$ seconds after the flaps have closed. The vortex pair is propogating to the left. In this experiment, tape has been applied to force the the natural wavelength of the instability to produce a clearer result.

with the experimental observations of [7]. Additionally, they found that the zigzag stability should behave as $F_v \sim \mathcal{O}(1)$, i.e. $L_v \sim U/N$. This length is known as the buoyancy length scale (cite) and has proven to be a very important length scale in stratified fluid flow, as we shall discuss below. This derivation of the buoyancy length scale, however, should be treated with some care since Billant and Chomaz assumed that $F_v \ll 1$ and showed that $F_v \sim \mathcal{O}(1)$.

In the final paper, Billant and Chomaz conducted a numerical linear stability analysis of the zigzag instability [9]. In this study, they numerically solved the linear Boussinesq equations for the growth rate of the leading eigenmode for specific wavenumbers. We will not discuss the results details of the paper here as their paper forms the basis for much of this thesis and we will rederive and discuss their results throughout the next three chapters. In the remainder of this chapter we derive the numerical equations that Billant and Chomaz used in [9] and provide some more background information. In Chapter 3 we introduce and discuss the numerical technique of spectral methods used to solve the numerical equations. In Chapter 4 we extend the analysis of Billant and Chomaz to length scales well below the sub-buoyancy scale of $L_b \sim U/N$.

1.4 Formulation of the Linear Problem

Following Billant and Chomaz [9], we consider the non-dimensional Boussinesq approximation to the Navier-Stokes equations in Cartesian co-ordinates

$$\frac{D\boldsymbol{u}}{Dt} = -\nabla p - \rho' \hat{\boldsymbol{e}}_z + \frac{1}{Re}\nabla^2 \boldsymbol{u}, \tag{1.34}$$

$$\nabla \cdot \boldsymbol{u} = 0, \tag{1.35}$$

$$\frac{D\rho'}{Dt} - \frac{w}{F_h^2} = \frac{1}{ReSc}\nabla^2 \rho', \tag{1.36}$$

where $D/Dt = \partial/\partial t + \boldsymbol{u} \cdot \nabla, \boldsymbol{u} = (u, v, w)$ is the velocity, p is the pressure, and ρ' is the density perturbation. We have non-dimensionalised by the characteristic velocity U, length R, time-scale R/U, pressure $\rho_0 U^2$, density $\rho_0 U^2/gR$, and defined $Sc = \nu/D$ as the Schmidt number, where D is the mass diffusivity, ρ_0 is the background density, and g is the gravitational constant. The Reynolds and horizontal Froude number are as defined above. The buoyancy frequency N, and hence the Froude number F_h, is assumed to be constant.

In order to investigate the linear growth rate, we proceed as the introduction and

expand the full velocity field as the sum of a basic state and a perturbation state.

$$\boldsymbol{u} = \boldsymbol{u}_0 + \tilde{\boldsymbol{u}} \tag{1.37}$$

$$p = p_0 + \tilde{p} \tag{1.38}$$

$$\rho' = \rho'_0 + \tilde{\rho}' \tag{1.39}$$

here the basic state is the Lamb-Chaplygin dipole which we will now discuss and explain how it provides a convenient theoretical model for the experiment by Billant and Chomaz [7].

1.4.1 The Lamb-Chaplygin Dipole

As the basic state for linear stability analysis we use the Lamb-Chaplygin dipole in a comoving frame [29]. This dipole is a solution to the 2D inviscid Euler equations. This basic state is motivated by numerous laboratory experiments[7, 25], as discussed above, which demonstrated that a vertically oriented Lamb-Chaplygin dipole is a good approximation to the vortex generated by two flaps closing in a tank of salt-stratified water. The dipole, in cylindrical coordinates, is given by the stream function

$$\psi_0(r,\theta) = \begin{cases} -\dfrac{2}{\mu_1 J_0(\mu_1)} J_1(\mu_1 r)\sin\theta & r \le 1, \\ -r\left(1 - \dfrac{1}{r^2}\right)\sin\theta & r > 1, \end{cases} \tag{1.40}$$

and the corresponding vertical vorticity $\omega_{z0} = \nabla_h^2 \psi_0$

$$\omega_{z0}(r,\theta) = \begin{cases} \mu_1^2 \psi_0(r,\theta) & r \le 1, \\ 0 & r > 1, \end{cases} \tag{1.41}$$

where J_0, J_1 are the zero and first order Bessel functions, $\mu_1 \approx 3.8317$ is the first root of J_1, and ∇_h is the horizontal Laplacian. The basic state velocity is purely horizontal and is given by $\boldsymbol{u}_{h0} = \nabla_h \psi_0 \times \hat{\boldsymbol{e}}_z$. Recall that in the previous section, Billant and Chomaz found experimentally that $\omega = k^2\psi$ where $k = 1.15$. Here we have that $\omega_{z0} = \mu_1^2 \psi_0$. If we consider the dimensional version, we would have that $k^2 = \mu_1^2/R^2$ where $R = 3.6$ cm. This gives $k^2 = 1.13$ cm^{-2} which corresponds very well with the experimental value of 1.15. Fig. 1.2 is a plot of the vorticity.

Let us now discuss the derivation of this result, which was first written down by Lamb and investigated further, independently, by Chaplygin. Although Lamb was the first to

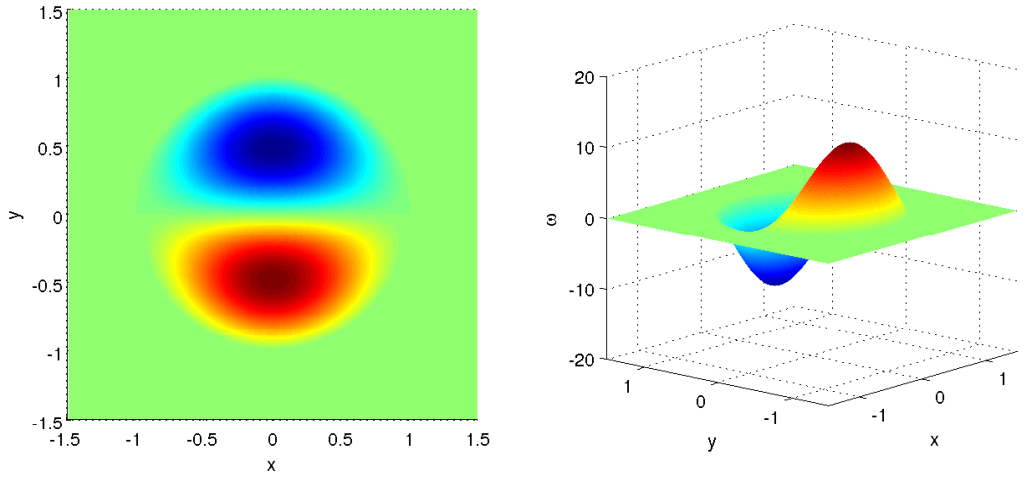

Figure 1.2: The Lamb-Chaplygin dipole.

write down the above solution to the Euler equations, he did not provide any motiviation for the derivation beyond it being an exact solution of the 2D steady Euler equations. However, a decade later, Lamb provided a slightly more in depth derivation motivating somewhat the study of this dipole. Independently, in Russia, Chaplygin provided a complete derivation and motivation for studying this dipole, although it remained unknown outside of Russia. Following [29] we repeat the key points of Chaplygin's argument.

Recall that the steady 2D Euler equations can be written in terms of the streamfunction ψ and a vorticity ω as

$$\nabla^2\psi = -\omega. \tag{1.42}$$

To choose ω, Chaplygin was motivated by the situation where we have a continuous vortex whose outer region is steady irrotational flow while the inner region is a translating vortex. Recall that the potential function for a flow outside a cylinder is

$$\psi = v_0\left(r - \frac{a^2}{r}\right)\sin\theta, \tag{1.43}$$

where a is the radius of the dipole and v_0 is the propogation velocity.

Inside the radius a, Chaplygin chose the vorticity to be $\omega = n^2\psi$ where n is a constant. In polar coordinates (1.42) becomes

$$\frac{\partial^2\psi}{\partial r^2} + \frac{1}{r}\frac{\partial\psi}{\partial r} + \frac{1}{r^2}\frac{\partial^2\psi}{\partial\theta^2} = n^2\psi \tag{1.44}$$

which we can guess at a solution of the form $\psi(r,\theta) = Z(r)\sin\theta$. Although Chaplygin did not provide specific motivation for choosing this specific vorticity, the above equation has a form that is similar to the irrotational flow outside the dipole and this makes the matching conditions simple. The resulting equation for $Z(r)$ is the well known Bessel equation (cite some book) and after grinding through the algebra, one obtains (1.40). Chaplygin also investigated the resulting pressure field produced by the dipole and was able to compute the circulation of the dipole. Unlike Lamb, he also considered a generalisation of the above where the dipole is no longer symmetric about the x-axis. The corresponding vorticity in this case is given by

$$\omega = n^2(\psi - \lambda) \tag{1.45}$$

where λ is an arbitrary parameter where $\lambda = 0$ is a completely symmetric dipole and $\lambda \to \infty$ corresponds to a completely asymmetric dipole. Here, again, Chaplygin investigated fully the pressure and circulation produced by this dipole. Additionally, in the same set of papers, Chaplygin also investigated the case of the dipole in rotating fluid, which was independently rediscovered 80 years later. Full details of this derivation are in [29] (flierl et. al)

1.5 Scaling Analysis (to be finished)

We have mentioned two dimensionless numbers in stratified flow, the Reynolds number and the Froude number. Both these dimensionless numbers arise when comparing the relative sizes of various terms in the Navier-Stokes equations. Depending on what aspect of a problem we are looking at, these numbers can appear in different places when we choose different scalings. We will now discuss some of the scaling arguments that have been used in stratified flow as it can provide insights into what mechanisms underlie the transition to and evolution of turbulence. A comprehensive review of scaling in stratified turbulence is provided in a recent review by Riley and Lindborg [40] and we will discuss the important scaling arguments therein.

For reference, we reproduce the Boussinesq equations here

$$\frac{\partial \mathbf{u}_h'}{\partial t'} + \mathbf{u}_h' \cdot \nabla_h' \mathbf{u}_h' + u_z' \frac{\partial \mathbf{u}_h'}{\partial z'} = -\frac{1}{\rho_0} \nabla_h' p' + \nu \nabla'^2 \mathbf{u}_h, \tag{1.46}$$

$$\frac{\partial u_z'}{\partial t'} + \mathbf{u}_h' \cdot \nabla_h' u_z' + u_z' \frac{\partial u_z'}{\partial z'} = -\frac{1}{\rho_0} \frac{\partial p'}{\partial z'} - \frac{\rho' g}{\rho_0} + \nu \nabla'^2 u_z, \tag{1.47}$$

$$\nabla_h' \cdot \mathbf{u}_h' + \frac{\partial u_z'}{\partial z'} = 0, \tag{1.48}$$

$$\frac{\partial \rho'}{\partial t'} + \mathbf{u}_h' \cdot \nabla_h' \rho' + u_z' \frac{\partial \rho'}{\partial z'} + \frac{\partial \rho}{\partial z'} u_z' = D \nabla^2 \rho', \tag{1.49}$$

where the primed quantities denote the dimenional quantities.

As a starting point, we produce a scaling argument that seperates the horizontal and vertical directions. As we saw in the experiment of Billant and Chomaz [7], in the zigzag instability there was a clear seperation between the vertical and horizontal scales. This difference in the vertical and horizontal directions suggests defining two length scales, the horizontal length scale L_h and the vertical length scale L_v. Associated with this seperation we introduce the horizontal velocity scale U and the vertical velocity scale V. The resulting scaling is

$$x' = L_h x, \qquad y' = L_h y, \qquad z' = L_v z, \qquad \mathbf{u}_h' = U \mathbf{u}, \qquad u_z' = V u_z \tag{1.50}$$

We also define another useful quantity that plays an important role in the scaling of stratified flows, the aspect ratio

$$\delta = \frac{L_v}{L_h}, \tag{1.51}$$

which measures how anisotrophic the length scales are. For the time scale, we choose the advective time scale

$$t' = \frac{L_h}{U} t, \tag{1.52}$$

which is the characteristic time of a vortex to be advected around the characteristic length [39, 10, 27]. Following these references the pressure and density scales are

$$p' = \rho_0 U^2 p, \qquad \rho' = \frac{U^2 \rho_0}{g L_v} \rho''. \tag{1.53}$$

The only quantity left unspecified is the vertical velocity which can be determined by setting the terms in the density equation to be the same order which yields

$$u_z' = u\frac{F_h^2}{\delta}u_z \tag{1.54}$$

This scaling now leads to the following set of equations [40]

$$\frac{\partial \mathbf{u}_h}{\partial t} + \mathbf{u}_h \cdot \nabla_h \mathbf{u}_h + \frac{F_h^2}{\alpha^2} u_z \frac{\partial \mathbf{u}_h}{\partial z} = -\nabla_h p + \frac{1}{\mathrm{Re}}\left(\nabla_h^2 \mathbf{u}_h + \frac{1}{\alpha^2}\frac{\partial^2 \mathbf{u}_h}{\partial z^2}\right), \tag{1.55}$$

$$F_h^2\left(\frac{\partial u_z}{\partial t} + \mathbf{u}_h \cdot \nabla_h u_z + \frac{F_h^2}{\alpha^2} u_z \frac{\partial u_z}{\partial z}\right) = -\frac{\partial p}{\partial z} - \rho + \frac{F_h^2}{\mathrm{Re}}\left(\frac{1}{\alpha^2}\frac{\partial u_z}{\partial z^2} + \nabla_h^2 u_z\right) \tag{1.56}$$

$$\nabla_h \cdot \mathbf{u}_h + \frac{F_h^2}{\alpha^2}\frac{\partial u_z}{\partial z} = 0, \tag{1.57}$$

$$\frac{\partial \rho}{\partial t} + \mathbf{u}_h \cdot \nabla_h \rho + \frac{F_h^2}{\alpha^2} u_z \frac{\partial \rho}{\partial z} = u_z + \frac{1}{\mathrm{Re}Sc}\left(\frac{1}{\alpha^2}\frac{\partial^2 \rho}{\partial z^2} + \nabla_h^2 \rho\right) \tag{1.58}$$

where

$$\mathrm{Re} = \frac{UL_h}{\nu}, \qquad F_h = \frac{U}{L_h N}, \qquad Sc = \frac{\nu}{D} \tag{1.59}$$

Lilly was the first to write these equations down although he assumed istrophy, i.e. $\delta = 1$.

Let us now investigate the limit of strong stratification, i.e. $F_h \to 0$ but let us leave the behaviour of F_h/δ undetermined. Additionally, let us consider $\mathrm{Re} \gg 1$ so, for the purposes of the scale analysis, ignore them. This results in the following equations

$$\frac{\partial \mathbf{u}_h}{\partial t} + \mathbf{u}_h \cdot \nabla_h \mathbf{u}_h + \frac{F_h^2}{\alpha^2} u_z \frac{\partial \mathbf{u}_h}{\partial z} = -\nabla_h p + \frac{1}{\mathrm{Re}}\frac{1}{\alpha^2}\frac{\partial^2 \mathbf{u}_h}{\partial z^2}, \tag{1.60}$$

$$0 = -\frac{\partial p}{\partial z} - \rho \tag{1.61}$$

$$\nabla_h \cdot \mathbf{u}_h + \frac{F_h^2}{\alpha^2}\frac{\partial u_z}{\partial z} = 0 \tag{1.62}$$

$$\frac{\partial \rho}{\partial t} + \mathbf{u}_h \cdot \nabla_h \rho + \frac{F_h^2}{\alpha^2} u_z \frac{\partial \rho}{\partial z} = u_z + \frac{1}{\mathrm{Re}Sc}\frac{1}{\alpha^2}\frac{\partial^2 \rho}{\partial z^2} \tag{1.63}$$

It was initially assumed by Lilly [27] and Riley et. al [39] that as $F_h \to 0$ then so does

F_h/δ. Thus the resulting equations are

$$\frac{\partial \mathbf{u}_h}{\partial t} + \mathbf{u}_h \cdot \nabla_h \mathbf{u}_h = -\nabla_h p + \frac{1}{\mathrm{Re}} \frac{1}{\alpha^2} \frac{\partial^2 \mathbf{u}_h}{\partial z^2}, \tag{1.64}$$

$$0 = -\frac{\partial p}{\partial z} - \rho \tag{1.65}$$

$$\nabla_h \cdot \mathbf{u}_h = 0 \tag{1.66}$$

$$\frac{\partial \rho}{\partial t} + \mathbf{u}_h \cdot \nabla_h \rho = \frac{1}{\mathrm{Re} Sc} \frac{1}{\alpha^2} \frac{\partial^2 \rho}{\partial z^2} \tag{1.67}$$

These equations have been well known in the atmosopheric modelling community. Notice that in these resulting equations, the horizontal and vertical velocities have become almost completely decoupled. They are not completely decoupled because there is still depenedence through the pressure term. However this decoupling led Lilly to conjecture that stratified turbulence in the strong stratification limit will obey 2D turbulence [27]. (add link to review of 2D turbulence). 2D turbulence exhibits an inverse energy cascade however this has not been observed in stratified turbulence (cite stuff... add when nonlinear written).

Building on the work of Lilly [27] and Riley et. al. [39], Billant and Chomaz [10] modified the argument suggesting that in the limit of strong stratifications that instead $F_h/\delta \to 1$ as $F_h \to 1$. This scaling analysis leads to $L_v \sim U/N$ which is the result obtained for the zigzag instability.

$$\frac{\partial \mathbf{u}_h}{\partial t} + \mathbf{u}_h \cdot \nabla_h \mathbf{u}_h + u_z \frac{\partial \mathbf{u}_h}{\partial z} = -\nabla_h p + \frac{1}{\mathrm{Re}} \frac{1}{\alpha^2} \frac{\partial^2 \mathbf{u}_h}{\partial z^2}, \tag{1.68}$$

$$0 = -\frac{\partial p}{\partial z} - \rho \tag{1.69}$$

$$\nabla_h \cdot \mathbf{u}_h + \frac{\partial u_z}{\partial z} = 0 \tag{1.70}$$

$$\frac{\partial \rho}{\partial t} + \mathbf{u}_h \cdot \nabla_h \rho + u_z \frac{\partial \rho}{\partial z} = u_z + \frac{1}{\mathrm{Re} Sc} \frac{1}{\alpha^2} \frac{\partial^2 \rho}{\partial z^2} \tag{1.71}$$

The assumption that $F_h/\delta \to 1$ can be rewritten to state that $L_v \sim U/N$, which is the buoyancy scale. In this case, there is no decoupling between the horizontal and vertical directions.

1.5.1 Stratified Turbulence (to be written when nonlinear chapter is written)

In this final section of background a few results from stratified turbulence that are releveant to the zigzag instability are discussed. A complete discussion of the generation of and full blown stratified turbuelence is beyond the scope of these this thesis and instead we refer the reader to a recent review of recent theoretical, numerical, and experimental results by Riley and Lindborg.

Discuss some recent results in the nonlinear evolution and turbulence generating of the zigzag instability.

References

[1] David J Acheson. *Elementary fluid dynamics*. Oxford University Press, 1990.

[2] P. Augier and P. Billant. Onset of seconardy instabilities on the zigzag instability in stratified fluids. *J. Fluid Mech*, 682:120–131, 2011.

[3] P. Augier, J.-M. Chomaz, and P. Billant. Spectral analysis of the transition to turbulence from a dipole in stratified fluid. *J. Fluid. Mech*, 713:86–108, 2012.

[4] B.J. Bailey. Three-dimensional instability of elliptical flow. *Phys. Rev. Lett.*, 57:2160, 1986.

[5] G.K. Batchelor. *An Introduction to Fluid Dynamics*. Cambridge University Press, 1967.

[6] P. Billant, P. Brancher, and J.-M. Chomaz. Three-dimensional stability of a vortex pair. *Phys. Fluids*, 11:2069–2077, 1999.

[7] P. Billant and J.-M. Chomaz. Experimental evidence for a new instability of a vertical columnar vortex pair in a strongly stratified fluid. *J. Fluid Mech*, 418:167–188, 2000.

[8] P. Billant and J.-M. Chomaz. Theoretical analysis of the zigzag instability of a vertical columnar vortex pair in a strongly stratified fluid. *J. Fluid Mech*, 419:29–63, 2000.

[9] P. Billant and J.-M. Chomaz. Three-dimensional stability of a vertical columnar vortex pair in a stratified fluid. *J. Fluid Mech*, 419:65–91, 2000.

[10] P. Billant and J.-M. Chomaz. Self-similarity of strongly stratified inviscid flows. *Phys. Fluids*, 13(6):1645–1651, 2001.

[11] L. Bovard and M.L. Waite. Short wave vortex instability in stratified fluids. *Physics of Fluids*, Submitted.

[12] J.P. Boyd. *Chebyshev and Fourier Spectral Methods*. Dover books on mathematics. Dover Publications, 2001.

[13] G. Brethouwer, P. Billant, E. Lindborg, and J.-M. Chomaz. Scaling analysis and simulations of strongly stratified turbulent flows. *J. Fluid Mech*, 585:343–368, 2007.

[14] S.A. Orszag C.M. Bender. *Advanced Mathematical Methods for Scientists and Engineers*. Springer, 1999.

[15] Steven C Crow. Stability theory for a pair of trailing vortices. *AIAA journal*, 8(12):2172–2179, 1970.

[16] A. Deloncle, P. Billant, and J.-M. Chomaz. Nonlinear evolution of the zigzag instability in stratified fluids: a shortcut on the route to dissipation. *J. Fluid Mech*, 660:229–238, 2008.

[17] A. Deloncle, P. Billant, and J.-M. Chomaz. Three-dimensional stability of vortex arrays in a stratified and rotating fluid. *J. Fluid Mech*, 678:482–510, 2011.

[18] P.G. Drazin and W.H. Reid. *Hydrodynamic Instability*. Cambridge University Press, 2004.

[19] Dale R. Durran. *Numerical Methods for Fluid Dyanimcs 2nd Edition*. Springer, 2010.

[20] Matteo Frigo and Steven G Johnson. The design and implementation of fftw3. *Proceedings of the IEEE*, 93(2):216–231, 2005.

[21] D.A. Herbert and S.M. de Bruyn Kops. Predicting turbulence in flows with strong stable stratification. *Phys. Fluids*, 18:18–28, 2006.

[22] R. Kerswell. Elliptical instability. *Annu. Rev. Fluid Mech.*, 34:83–113, 2002.

[23] Kundu. *Fluid Dynamics 5th Edition*. Academic Press, 2012.

[24] M. Lesieur. *Turbulence in Fluids*. Springer, 2008.

[25] T. Leweke and C.H.K. Williamson. Cooperative elliptic instability of a vortex pair. *J. Fluid Mech*, 360:85–119, 1998.

[26] T. Leweke and C.H.K. Williamson. Long-wavelength instability and reconnection of a vortex pair. In E. Krause and K. Gersten, editors, *IUTAM Symposium on Dynamics of Slender Vortices*, volume 44 of *Fluid Mechanics and Its Applications*, pages 225–234. Springer Netherlands, 1998.

[27] D.K. Lilly. Stratified turbulence and the mesoscale variability of the atmosphere. *J. Atmos. Sci*, 40:749, 1983.

[28] E. Lindborg. The energy cascade in a strongly stratified fluid. *J. Fluid Mech*, 550:207–242, 2006.

[29] V.V. Meleshko and G. J. F. van Heijst. On Chaplygin's investigations of two-dimensional vortex structures in an inviscid fluid. *J. Fluid Mech*, 272:157–182, 1994.

[30] C. Meyer. *Matrix Analysis and Applied Linear Algebra Book and Solutions Manual*. Matrix Analysis and Applied Linear Algebra. Society for Industrial and Applied Mathematics, 2000.

[31] T. Miyazaki and Y. Fukumoto. Three-dimensional instability of strained vortices in a stably stratified fluid. *Phys. Fluids A*, 4:2515–2522, 1992.

[32] Saffman PG. Moore DW. The instability of a straight vortex filament in a strain field. *Proc. R. Soc. Lond. A*, 346:413–425, 1975.

[33] K. Ngan, D.N. Straub, and P. Bartello. Aspect ratio effects in quasi-two-dimesional turbulence. *Phys. Fluids*, 17:1–10, 2005.

[34] P. Otheguy, P. Billant, and J.-M. Chomaz. Elliptic and zigzag instabilities on co-rotating vertical vortices in a stratified fluid. *J. Fluid Mech*, 553:253–272, 2006.

[35] Orzag Peterson. Numerical simulation... *collection*, 66614914:1–1000, 1972.

[36] R.T. Pierrehumbert. Universal short-wave instability of two-dimensional eddies in an inviscid fluid. *Phys. Rev. Lett*, 57(17):2157–2159, 1986.

[37] Osborne Reynolds. An experimental investigation of the circumstances which determine whether the motion of water shall be direct or sinuous, and of the law of resistance in parallel channels. *Proceedings of the Royal Society of London*, 35(224-226):84–99, 1883.

[38] J.J. Riley and S. M. de Bruyn Kops. Dynamics of turbulence strongly influenced by buoyancy. *Phys. Fluids*, 15(7):2047–2059, 2003.

[39] J.J. Riley and M.-P. Lelong. Fluid motions in the presence of strong stable stratifications. *Annu. Rev. Fluid Mech.*, 32:613–657, 2000.

[40] J.J. Riley and E. Lindborg. Recent progress in stratified turbulence. In K. Sreenivasan P. Davidson, Y. Kaneda, editor, *Ten Chapters in Turbulence*. Cambridge University Press, 2013.

[41] Lloyd N. Trefethen. *Spectral Methods in MATLAB*. SIAM, 2000.

[42] D.J. Tritton. *Physical Fluid Dynamics*. Oxford Science Publications. Clarendon Press, 1988.

[43] Widnall SE Tsai C-Y. The stability of short waves on a straight vortex filament in a weak externally imposed strain field. *J. FLuid Mech*, 73:721–733, 1976.

[44] G.K. Vallis. *Atmospheric and Oceanic Fluid Dynamics: Fundamentals and Large-scale Circulation*. Cambridge University Press, 2006.

[45] Milton Van Dyke. *Perturbation Methods in Fluid Mechanics*. Parabolic Press Stanford, 1975.

[46] Milton Van Dyke. *An Album of Fluid Motion*. Parabolic Press Stanford, 1982.

[47] M.L. Waite. Stratified turbulence at the buoyancy scale. *Phys. Fluids*, 23:23–35, 2012.

[48] M.L. Waite and P. Bartello. Stratified turbulence dominated by vortical motion. *J. Fluid Mech*, 517:281–301, 2004.

[49] M.L. Waite and P.K. Smolarkiewicz. Instabilty and breakdown of a vertical vortex pair in a strongly stratified fluid. *J. Fluid Mech.*, 606:239–273, 2008.

[50] R.M. Wald. *General Relativity*. University of Chicago Press, 2010.

[51] F. Waleffe. On the three-dimensional instability of strained vortices. *Phys. Fluids A*, 3:76, 1990.

[52] S.E. Widnall, D.B. Bliss, and C.Y. Tsai. The instability of short waves on a vortex ring. *J. Fluid Mech*, 66:35, 1974.